"Naked" gold nanoparticles as colorimetric reporters for biogenic amine detection

Annamaria Lapenna[1]*, Marcella Dell'Aglio[2] , Gerardo Palazzo[1, 3], Antonia Mallardi[4]*

[1] Chemistry Department, University of Bari 'Aldo Moro', via Orabona 4, 70125 Bari, Italy
[2] CNR-NANOTEC, Institute of Nanotechnology, c/o Chemistry Department, Via Orabona 4, 70125 Bari, Italy
[3] CSGI (Center for Colloid and Surface Science) c/o Chemistry Department, via Orabona 4, 70125 Bari, Italy
[4] CNR-IPCF, Institute for Chemical-Physical Processes, c/o Chemistry Department, via Orabona 4, 70125 Bari, Italy

* **Corresponding authors**:
Antonia Mallardi
CNR-IPCF, National Research Council, Institute for Chemical-Physical Processes, c/o Chemistry Department, via Orabona 4, 70125 Bari, Italy.
Tel +39-080-5442226
a.mallardi@ba.ipcf.cnr.it

Annamaria Lapenna
Chemistry Department, University of Bari 'Aldo Moro', via Orabona 4, 70125 Bari, Italy
annamaria.lapenna@uniba.it

Highlights

- "Naked" gold nanoparticles (AuNPs) have been employed for biogenic amine sensing.
- A fast and simple AuNPs colorimetric assay is proposed.
- The assay is based on AuNPs aggregation induced by histamine.
- The method has been applied for the determination of biogenic amine content in wine.
- An interaction mechanism between AuNPs and histamine is proposed.

Keywords: biogenic amines, histamine, naked gold nanoparticles, laser ablation in liquid, colorimetric assay, amine sensing

Graphical abstract

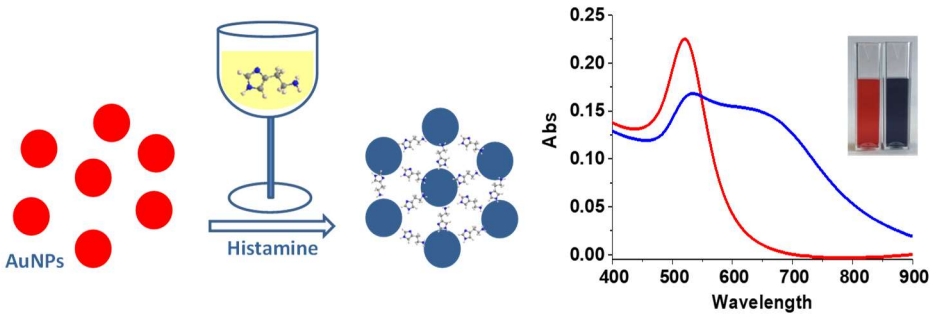

ABSTRACT

Biogenic amines (BA) are present in fermented foods and beverages. As their high intake may produce adverse reactions in humans, the control of BA concentration is advisable. Simple, rapid, point-of-use analytical platforms are needed because traditional methods for the detection and quantification of BAs are expensive and time-consuming.

In this work a colorimetric assay based on “naked” gold nanoparticles (AuNPs) which is sensitive to BAs is developed. The detection is based on the AuNPs aggregation upon binding of the analytes. Aggregation induced a change in color of the solution from burgundy to grey/blue. Concomitantly, UV–vis absorption spectra of AuNPs showed that the characteristic absorption peak at 520 nm decreased and a new absorption peak was generated at 650 nm. So, analyte detection can be achieved by eye and quantification can be simply obtained by using a spectrometer. The response characteristics of the assay have been determined using histamine (His) as BA model molecule. The assay has a limit of detection of 0.2 μM. The BA content in wine was determined by the assay.

Finally, as AuNPs have been prepared by LAL in absence of any capping agent, a mechanism of aggregation based on the direct interaction between the amine groups of His with gold is proposed.

1. Introduction

Biogenic amines (BAs) are low molecular weight organic bases with an aliphatic (putrescine, cadaverine, spermine, spermidine) aromatic (tyramine, phenylethylamine) or heterocyclic (histamine, tryptamine) structure. They are usually formed by the decarboxylation of amino acids and play important roles in several physiological functions like as human brain activity, regulation of blood temperature or cell growth and differentiation. Despite their regulatory function in physiological processes, at high concentration BAs may have toxic effects in organisms, inducing adverse reactions such as nausea, headaches and changes in blood pressure [1]. BAs at low concentrations occur naturally in food, especially fish and meat, and drinks as wine and beer, but they can be also formed during storage. Since any food material produced by fermentation or exposed to microbial contamination during processing or storage may contain BAs, their concentration is linked to the degree of preservation, good-processing or degradation of the food. For this reason, BAs are considered to be markers of freshness and hygiene during storage. So, the detection of the BA in food is of interest both for toxicological reasons, since high levels of dietary BA can be toxic, and for their role as possible quality indicators.

The quantification of BAs in food samples has mainly been performed by chromatographic techniques, such as high-performance liquid chromatography (HPLC), gas chromatography (GC) and thin layer chromatography (TLC), or by capillary electrophoresis (CE) methods [2, 3]. These methods are laborious, time consuming and requires expensive instrumentation, thus, new methods are needed to achieve rapid, accurate, reproducible and low-cost detection. Recently, particular attention is devoted to nanosensors development.

Nowadays, metallic nanoparticles, especially Au nanoparticles (AuNPs), have been favorably selected to design novel sensors for fast, cost-effective, and accurate analysis in environmental and biological samples [4]. Colorimetric assays based on AuNPs have been designed exploiting their high stability, facile synthesis, excellent biocompatibility and strong Surface Plasmon Resonance (SPR) [5,6]. Depending on the size of AuNPs, controlled aggregation of the particles can result in color change, from red to purple to blue. The unique SPR properties and the colors associated with the aggregation and dispersion of the colloidal particles make AuNPs ideal colorimetric reporters for biological analysis.

Recently, an immunochromatographic test exploiting both magnetic and AuNPs has been proposed for the quantification of histamine [7]. Moreover, colorimetric assays based on AuNPs have been used to quantify histamine [8, 9, 10] and other amine (dopamine [11], melamine [12, 13]). In all those approaches, citrate-capped AuNPs (as prepared or modified) were used. These AuNPs are stabilized by a layer of negatively charged citrate ions which keep the nanoparticles separated and stable in aqueous solution. Addition of analytes causes AuNPs aggregation that will remarkably alter the extinction spectrum and the color of AuNPs, which sometimes can be distinguished by bare eyes.

In the above mentioned articles the authors hypothesize that the amine-induced aggregation could be due to an electrostatic interaction between the positively charged amine groups and the negatively charged citrate groups of the NPs or to an exchange between citrate ions and amines which are able to bind directly the NPs. Overall, the details of the interactions which leads to the formation of AuNPs aggregates have not been clarified.

In this paper we first investigate the mechanism of amine-induced AuNP aggregation to ascertain that this is a specific effect of amines and not a mere electrolyte-induced destabilization of colloid particles. To this end we use “naked” AuNPs, synthesized by laser ablation in liquid (LAL). LAL technique performed in water

allows the synthesis of metal NPs free from any capping layer [14, 15]. The lack of any kind of stabilizer makes these NPs interesting for different applications and research fields [16, 17, 18, 19, 20,21], since it is possible to directly test their surface reactivity. As a matter of fact, “naked” AuNPs can represent a valid model system to study the interactions with amines without the interference due to the presence of capping agents. The present study demonstrates that BAs specifically promote the aggregation of nanoparticles at such low concentrations that the effect of most interferents is negligible. Subsequently, these pieces of information have been successfully used to develop a simple colorimetric method for the determination of BA in wine.

2. Materials and Methods

2.1 AuNP synthesis by laser ablation

AuNPs are produced by LAL by employing a ns NdYAG (Quanta System PILS-GIANT) with a pulse duration of 8 ns, a 1064 nm laser wavelength with a fluence of 64 J/cm2 and a laser frequency of 10 Hz. With a plano convex lens of 5 cm focal length, the laser was focused on Au target located on the bottom of a cuvette filled with 3 mL of KCl 100 μM (prepared using milliQ water). The focal plane of the laser beam was put inside the target, in order to get a laser crater on the target surface with a diameter of 1 ± 0.2 mm. The gold target was purchased from Kurt J. Lesker Company.

2.2 AuNP characterization

AuNPs solutions were characterized by dynamic light scattering (DLS) and by Laser Doppler Electrophoresis (LDE) measurements using a Zetasizer-Nano ZS from Malvern Instruments. DLS measurements were performed in backscattering at a fixed detector angle of 173°, with the cell holder maintained at 25°C by means of a Peltier element.

The LDE measurements were performed at the stationary levels of a capillary cell and the scattered light was collected in forward scattering at a fixed detector angle of 17°; the average electrophoretic mobility was retrieved with a fast field reversal (FFR) sequence (high frequency alternating electric field) while the distribution of electrophoretic mobilities has been obtained using slow electric field reversal (SFR) sequence.[22] The ζ-potential was subsequently evaluated from the electrophoretic mobility according to the Hückel approximation.

The Vis spectrum of AuNPs in the region between 350 and 950 nm was registered using an Agilent 8453 UV–Visible diode-array spectrophotometer. The absorbance value at the wavelength of the surface plasmon is employed to estimate the NPs concentration. To obtain the extinction coefficient at the maximum of absorbance, that also depends on the NPs size, calibration curves described elsewhere [23] are used.

2.3. Colorimetric histamine assay

Histamine, from Sigma-Aldrich, was solubilized at different pH values using: Citrate buffer at pH=5.4, Phosphate buffer at pH=7.4, Carbonate buffer at pH=11 in order to obtain the three protonation forms of histamine. In all the cases a buffer concentration of 20 mM was used. AuNPs were dispersed in HPLC water. In a typical experiment, 500 μl of histamine solution at the desired concentration in the suitable buffer were added to 500 μl of AuNPs at room temperature. 10 minutes after mixing the sample was subjected to UV-vis absorption, DLS and LDE measurements. The final buffer concentration of 10 mM, obtained in the

sample, does not induce aggregation of the AuNPs. In fact, control experiments (blanks) performed in the same way but in absence of histamine show that AuNPs remain stable in buffer for more than 24 hours.

The aggregation index (AI) was determined as the ratio between the sum of the absorbance at 650 nm and at 900 nm with respect to the absorbance at 520nm

$$AI = \frac{Abs@650\ nm + Abs@900nm}{Abs@520nm} \qquad (1)$$

2.4. Real sample analysis

Table white wine was acquired from a local supermarket. It was diluted with buffer in the required ratios and then 500 μl of each dilution were added to 500 μl of 2 nM AuNPs. Absorbance spectra were collected 10 min after mixing and the AI values were evaluated according to eq. 1. The comparison with the calibration curve is detailed in section 3.2.

3. Results and Discussion

We have focused our study on AuNPs synthesized by means of the laser ablation in water of a solid gold target that leads to the formation of "naked" metallic gold particles free from any capping layer [14]. These AuNPs have an average size of 18 nm and a negative (-64 mV) ζ-potential (one should take into account that, due to the very small size of these particles and to the low ionic strength of these experiments, the most appropriate approximation in passing from electrophoretic mobility to ζ-potential values is the Hückel equation).

As a model of biogenic amine we have chosen the histamine (His) because it has advantages from an experimental point of view (at used concentrations it doesn't stink) and it deserves attention because of its role as a neurotransmitter and its involvement in the allergic inflammatory reactions [3, 24]. Moreover, histamine is the only BA for which legal limits in foods have been fixed or maximum values in wine have been recommended [25, 26].

3.1 Interaction of AuNPs and histamine

Histamine can exist in three different forms depending on the pH to which it is solubilized (**Scheme 1**). Under physiological conditions, the aliphatic amino group (having a pKa ≈ 9.4) will be protonated, whereas the second nitrogen of the imidazole ring (pKa ≈ 5.8) will not be protonated. Under physiological conditions, histamine is in form of monovalent cation. Under acid conditions, it is characterized by a dicationic form because both the aliphatic amino group and nitrogen of the imidazole ring will be protonated. Whereas under basic conditions, histamine is in a neutral form with both the aliphatic amino group and the nitrogen of the imidazole ring non-protonated[25].

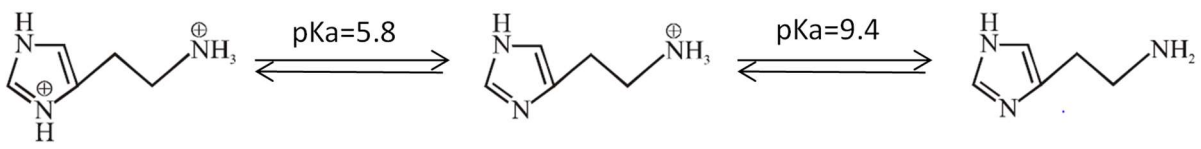

Scheme 1. *Different protonation forms of histamine.*

It is not clear if the interaction between AuNPs and histamine occurs via electrostatic or chemical interaction. The electrostatic interaction should involve the protonated amino group of histamine and negatively charged AuNPs, while chemical interaction should involve gold surface and amino functionalities. Therefore, we investigated the interaction between AuNPs and histamine at pH= 7.4, where histamine is in a cationic form, and at pH= 11, where it is in its uncharged form. A set of experiments has been performed leaving fixed the histamine concentration at 1 μM and increasing the AuNPs concentration from 0.5 nM to 8 nM.

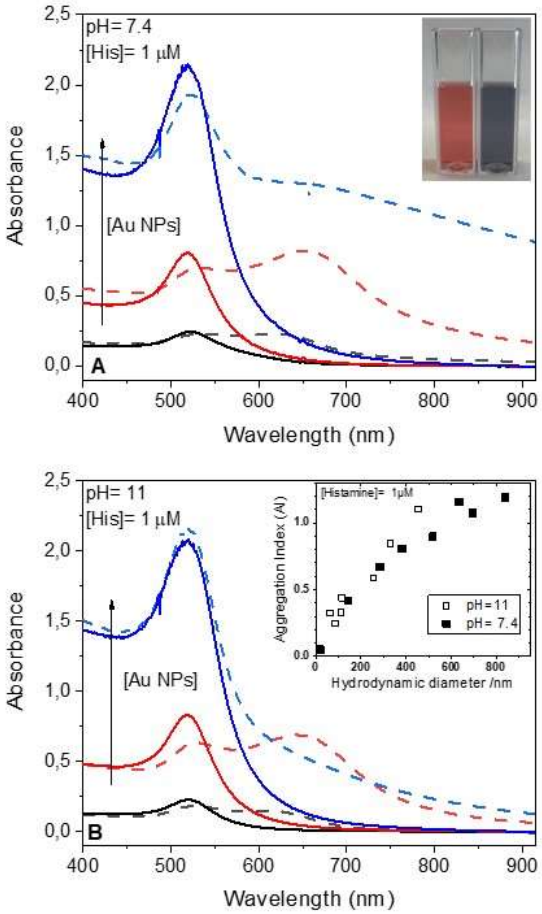

Fig. 1. *Visible spectra of AuNPs in absence (solid lines) and presence (dashed lines) of 1 μM histamine; AuNPs concentrations are 0.5 (black), 2 (red) and 6 (blu) nM. A) pH= 7.4; Inset: picture of the solution of AuNP 2 nM with (right) and without (left) 1 μM histamine. B) pH= 11; Inset: dependence of the aggregation index (eq. 1) on the size of the aggregates measured by DLS at two pH values (DLS data are from Fig.2).*

For each AuNPs-histamine sample, we have prepared a "control" sample in which AuNPs are mixed with buffer without histamine. For all control samples, AuNPs-buffer solutions have a burgundy color that does not change with time. UV–vis absorption spectra measured 24 hours after mixing showed that the characteristic absorption peak at 520 nm remains unchanged, indicating that nanoparticles are stable in buffer solutions.

After histamine addition to AuNPs, in all conditions tested, solutions changed their color from burgundy to blue and then to gray, evidencing that histamine can induce the aggregation of AuNPs. An example is shown in the inset of **Fig. 1A**. Such color changes reflect the shift of the gold surface plasmon resonance

(SPR) due to the formation of clusters. Indeed, the absorption spectra reveal the formation of a second SPR band centered around 650 nm. The width of such a band increases upon increasing the concentration of AuNP extending to higher wavelengths. As an example, in **Fig. 1** visible spectra of AuNPs, at pH= 7.4 and pH= 11, in absence and in presence of 1 μM histamine are shown. For a better readability of the figure, only spectra related to few of the explored concentrations of nanoparticles are shown (namely 0.5, 2 and 6 nM).

Parallel DLS measurements demonstrate a dramatic increase in the hydrodynamic size of the objects present in solution due to the formation of aggregates (see **Fig. 2**). Since sizing via DLS is performed using an expensive instrumentation, it is useful to exploit the change in the visible spectrum to have a quantitative index of aggregation that could be obtained from inexpensive absorbance measurements.

In order to have an Aggregation Index (AI) that monotonically increases passing from null to high aggregation we propose to divide the sum of absorbance values at 650 nm (reflecting mainly oligomers) and at 900 nm (mainly due to large aggregates formed) by the absorbance at 520 nm (reflecting monomeric AuNP) according to **Eq. 1** in the experimental section.

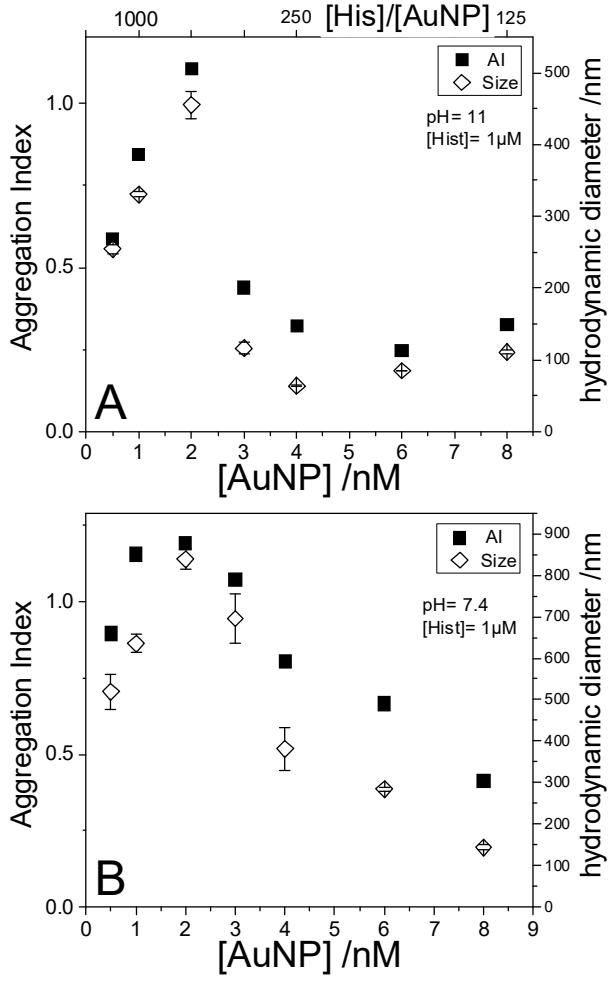

Fig. 2. *Aggregation Index (left ordinate) and hydrodynamic diameter (right ordinate) of AuNPs at different concentration and in the presence of 1 μM histamine. Error bars are the standard deviation of at least three replicates. A) data at pH= 11. In the top abscissa the mole ratios histamine/AuNPs are shown. B) data at pH= 7.4.*

In **Fig. 2**, the AI values and the size of the aggregates formed at different AuNPs concentrations are shown. **Fig. 2A** reports results obtained at pH= 11. For AuNPs dispersed in buffer only (in absence of histamine) we measured an AI of 0.05. After mixing of AuNPs and histamine, aggregation of nanoparticles occurs. Increasing AuNPs concentration, the AI increases reaching a value of 1.1 (measured at 2 nM NPs), then decreases to a value of 0.3. A similar behavior is observed for the hydrodynamic diameter of aggregates which closely follows the trend registered for the AI: the diameter increases from ~20 nm (value measured for AuNPs alone) to 450 nm and then decreases to about 100 nm. At pH= 7.4 results obtained in terms of AI and DLS measurements show the same trend registered for pH= 11. The only difference is that at high AuNPs concentration larger aggregated are formed, characterized by an AI of 1.2 and a diameter of 850 nm (**Fig. 2B**). The parallel trends of aggregation index and size suggest that the AI values evaluated according to eq. 1 is a meaningful estimate of the AuNP aggregation. This is confirmed by plotting the AI vs. size for all the AuNP concentration and for both the pH. In such a graph, shown in the Inset of **Fig. 1B**, all the data follow the same master curve independently from the pH value and the nanoparticle concentration.

In order to evaluate the effectiveness of "naked" AuNPs, we performed a set of experiments using AuNPs synthesized following Turkevich's procedure [27]. This method leads to the formation of citrate-capped AuNPs with an average size of 50 nm and a negative (-45 mV) ζ-potential. In the experiments we left the histamine concentration fixed at 1 μM, increasing the AuNPs concentration from 0.5 nM to 2 nM. At both pH = 7.4 and 11, the interaction of histamine with citrate-capped AuNPs is very similar to what found for naked AuNP, then we show only the result obtained at pH=7.4. In **Fig. 3A** visible spectra of citrate-capped AuNPs in absence and in presence of 1 μM histamine are shown. Here again, histamine addition induces the red shift of the gold surface plasmon resonance, indicating the aggregation of AuNPs. **Fig. 3B** is a direct comparison of the AI values and the size of the aggregates formed at different AuNPs concentrations and obtained using both types of AuNPs. The comparison in Fig. 3B indicates that citrate-capped AuNPs form bigger aggregates, in particular at low NPs concentration, than the corresponding "naked" AuNPs prepared by LAL. However, it should be taken into account that, due to the presence of an excess of citrate, the ionic strength of citrate-capped AuNPs solutions is unknown but reasonably greater than that of naked, accounting for the larger size found for citrate-capped AuNPs. At high AuNPs concentrations the differences in terms of both AI and size are reduced.

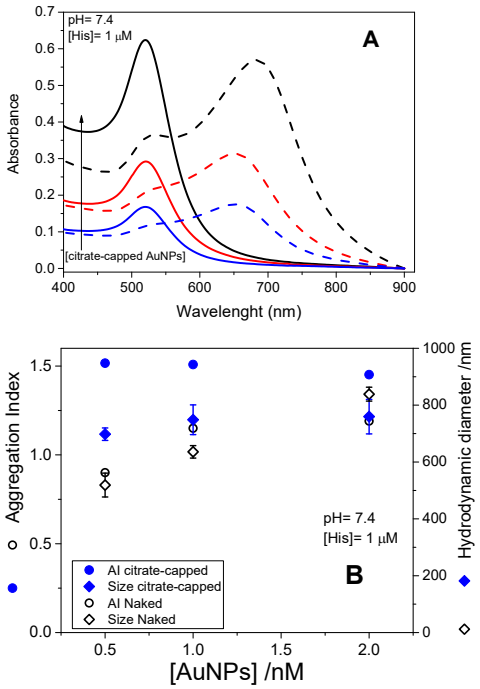

Fig. 3. *A) Visible spectra of citrate-capped AuNPs in absence (solid lines) and presence (dashed lines) of 1 μM histamine; AuNPs concentrations are 0.5 (blu), 1 (red) and 2 (black) nM. Data at pH= 7.4.*B) *Aggregation Index (left ordinate) and hydrodynamic diameter (right ordinate) of citrate-capped and naked AuNPs, at different concentration, and in the presence of 1 μM histamine. Data at pH=7.4 Error bars are the standard deviation of at least three replicates.*

The ζ-potential values of aggregates formed by naked AuNPs anf histamine are reported in **Fig. 4** together with values collected in acidic conditions (pH= 5). At the three pHs the pristine AuNPs are always negatively charged with a ζ-potential that becomes more negative going towards alkaline conditions (see the right ordinate in **Fig. 4**). Specifically the values are -42±7 mV at pH= 5, -54±4 mV at pH= 7.4 and -67±7 mV at pH= 11. Addition of histamine 1 μM triggers a large aggregation at all the pH and at all the concentrations but has only a negligible impact on the measured ζ-potentials.

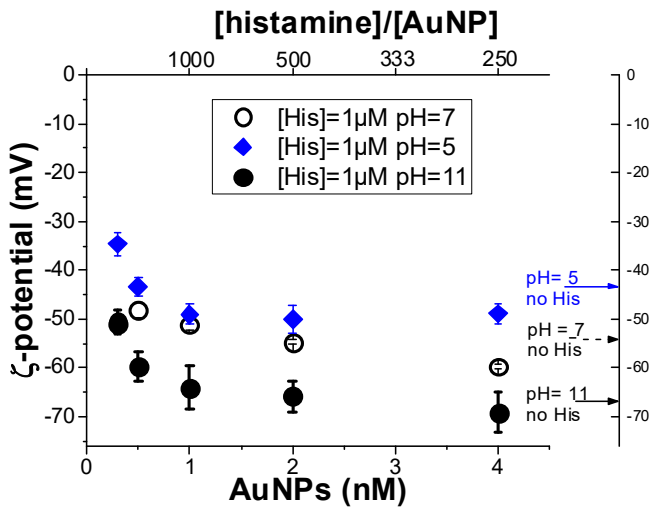

Fig. 4. *The ζ-potential values of AuNPs at different concentration and in the presence of 1 μM histamine. The top abscissa is the mole ratio histamine/AuNP. Error bars are the standard deviation of at least three replicates. Also shown on the right ordinate are the values in the absence of histamine. For the purpose of comparison also the values at pH=5 are shown.*

The behavior at pH 11 is a case in point. At this pH the pristine AuNPs are strongly negative and the histamine should be in its fully neutral form. Yet, upon addition of a tiny amount of histamine (1 μM), extensive and irreversible coagulation takes place with formation of aggregates (size ranging from 100 nm to 0.5 μm, **Fig. 2B**). However, for these samples, the measured ζ-potentials are always more negative than – 50 mV (see **Fig. 4**) a value that should assure high colloid stability at the low ionic strength of these experiments (after mixing histamine and AuNPs, the buffer concentration is 5 mM). Such evidences are sufficient to rule out any electrostatic origin of the coagulation and, of course, any mechanism that rests on the interaction between histamine and capping agents such as citrate.

Having excluded electrostatic mechanisms, the role played by histamine molecules in inducing the aggregation of "naked" nanoparticles (in the absence of capping agents) can be explained by taking into account an "interparticle crosslinking aggregation mechanism" [5] where an histamine molecule plays the role of a bidentate linker for two AuNPs. As already mentioned, histamine presents two different amine functionalities (an aliphatic amino group and an imidazole ring). It has been reported that either the two nitrogens of an imidazole ring [28] and the aliphatic amines [29], can bind the gold surface of nanoparticles. So, histamine molecules can actively participate to AuNPs aggregation process acting as crosslinkers.

The role of histamine as bidentate ligand accounts for the bell-shaped dependence of the aggregation with the AuNP concentration observed in the experiments of **Fig. 2**. Such a peculiar behavior can be explained by taking into account the evolution of ratio between histamine (at a fixed concentration of 1 μM in these experiments) and AuNPs (see **Scheme 2** for a pictorial representation).

When AuNPs concentration is low, the ratio [His]/[AuNP] is high and histamine molecules saturate the surface of all nanoparticles. Under these conditions the probability that an already bound histamine molecule will encounter another nanoparticle with an empty binding site is very low. Then, only small oligo aggregates are formed. Loading the system with further AuNPs decreases the [His]/[AuNP] ratio. The available histamine is not enough to saturate the gold surface and there are many free binding sites on the nanoparticles. These are the conditions for a dramatic growth of three-dimensional clusters (akin to a gel formation). Experimentally such a condition is fulfilled at a [His]/[AuNP] ratio of 500 (at [AuNP]= 2 nM), where the interaction between histamine and AuNPs is optimal. Eventually, a further increase of AuNPs concentration up to 8 nM reduces the number of histamine molecules bound per nanoparticle. For these sub-optimal [His]/[AuNP] ratios the probability to link several nanoparticles in the same aggregate decreases and for high enough AuNP concentration only dimers can form.

Scheme 2. *Pictorial representation of the possible interaction mechanism between histamine and AuNPs.*

Inspection of Fig. 2, indicates that the size of the aggregates is larger at pH =7.4 than at pH= 11. This is likely linked to the pH dependence of the histamine protonation state and of the surface charge of the AuNPs. The histamine binds the gold through non-electrostatic chemical interactions but, to do so, the molecule and the nanoparticles have to get in touch and such association kinetics are known to be very sensitive to the charges brought by the partners [30]. Accordingly, the presence of positive charges on histamine speeds-up its binding to the oppositely charged AuNPs. On the other hand, naked AuNPs are more negatively charged at alkaline than at neutral pH and their collision to negatively charged clusters is slowed down at high pH. Both the effects conspire to have faster aggregation rates (and therefore larger aggregates) at pH=7.4 compared to pH=11.

3.2. Colorimetric Assay of histamine

The AuNPs aggregation induced by histamine results in a color change from burgundy to blue/gray which might be monitored spectrophotometrically or even by naked eye. This aggregation, investigated in the previous section, is not due to a mere screening of the negative charges on the nanoparticles but to a specific chemical interaction between the histamine amino groups and the gold surface and is promising for its exploitation in a colorimetric assay for biogenic amines.

Accordingly, we have used the “Naked” AuNPs as colorimetric reporters for the presence of BAs, using histamine as model substrate. The assay is based on the relation between the extent of the AuNPs aggregation (expressed by means of the Aggregation Index) and the histamine concentration. In this instance the calibration curve was made keeping fixed the NPs concentration at 1 nM and varying the histamine concentration. The AI increased with the increase in the concentration of histamine, along with the color change from burgundy to blue and to gray. The variation could be visualized by the naked eyes as shown in upper panel of **Fig. 5**.

The corresponding dependence of the AI on the histamine concentration at pH= 7.4 is shown in the lower panel of **Fig. 5**. The above described mechanism of aggregation leads to a sigmoid dependence of the AI on the analyte concentration. Passing from 0.2 μM to 0.5 μM is enough to enter in the regime where an efficient aggregation takes place. A similar behavior is observed also at alkaline pH (inset of **Fig. 5**). Such a sigmoid trend has pros and cons. The fact that the change in color takes place at sub-micromolar concentration allows the use of the assay as a rapid screening for toxic concentration of BAs. The maximum level of histamine permitted for food consumption is around 1 mM [2]. This means that one can easily dilute a thousand times the sample thus removing the interference due to salts.

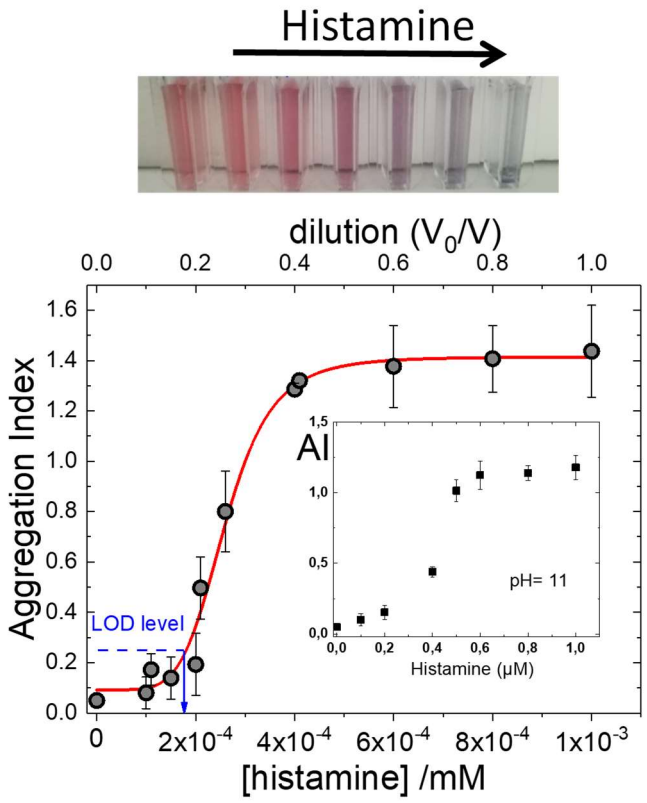

Fig. 5. *Aggregation Index as a function of the histamine concentration for AuNP 1 nM at pH= 7 (in the inset are shown the results of an analogous experiment at pH=11). The upper abscissa is the dilution ratio between the initial volume (V_0) of the stock solution at histamine concentration C_0= 1 μM and the actual volume of each sample. Error bars are the standard deviation of at least three replicates. The red curve is the fit to Eq. 2 using as independent variable V_0/V and keeping fixed C_0= 1 μM. the best-fit parameters are B= 1.32±0.08, offset= 0.09±0.05, K_d = 0.26±0.02 and n= 5.5±1.2. Also shown is the LOD level (offset + 3 times its standard deviation) and the corresponding LOD= 0.18 μM. The upper panel is a photograph of some of the samples used for the calibration.*

On the other hand, the step sigmoidal dependence of the AI on the analyte concentration poses problems to the use of a classical linear calibration curve. Here the dynamical range is limited to 0.2 μM < [His] < 0.4 μm. For higher analyte concentration the assay saturates and for lower concentration it doesn't respond. To circumvent this problem, we have developed an approach based on the use of different dilutions of the sample.

The calibration curve was built by fitting the experimental data to an analytical function that reproduce the sigmoid behavior. In this case we have chosen the Hill's equation often used to describe cooperative behavior:

$$AI = \frac{\left(\frac{V_0}{V}C_0\right)^n}{{K_d}^n + \left(\frac{V_0}{V}C_0\right)^n} B + offset \qquad (2)$$

Here the Hill's equation was used only to describe phenomenologically the experiments and the corresponding K_d and n parameters are not expected to have a physical meaning.

The calibration curve, in **Eq. 2**, is written as a function of the dilution, defined as the ratio between the initial (V_0) and the actual volume (V) and of the initial sample concentration (C_0). In the calibration step, the samples have been prepared from a stock solution at fixed concentration C_0 and the experimental data have been reported as a function of the dilution ratio V_0/V. This is shown in **Fig. 5** in the top abscissa.

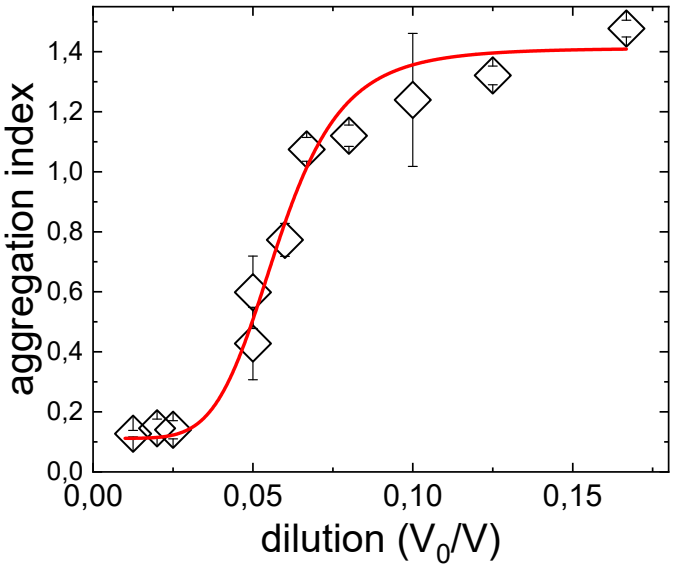

Fig. 6. *Real sample analysis. Aggregation Index as a function of the dilution ratio of a sample of wine. The data have been fitted to eq. 2 with fixed values: B= 1.32, offset= 0.09, K_d = 0.26 and n= 5.5. The only adjustable parameter was C_0. The red curve corresponds to the best fit value C_0= 4.5±0.1 μM. Error bars are the standard deviation of at least three replicates*

The data can be therefore fitted to **Eq. 2** keeping fixed the known C_0 and obtaining as best fit the values of the constant parameters listed in the caption of **Fig. 5**. The uncertainty on the *offset* value allows the evaluation of the Limit of Detection (LOD) as the concentration corresponding to an AI that is three times such uncertainty above the offset (see **Fig. 5** for a graphical representation). For the proposed assay the calculated LOD is 0.18 μM, a value in line or below those obtained by means of nanomaterials based optical sensors [25].

Once the constant parameters in **Eq. 2** have been assessed it is possible to fit data obtained along a dilution path of the same sample to **Eq. 2** leaving as the only adjustable parameter its unknown concentration C_0. This is shown in **Fig. 6** for a real sample of wine. The wine was directly diluted with Phosphate buffer in a ratio 1/5 and then further 10 dilutions have been done. Each dilution was assayed with the AuNP and the AI values have been plotted as a function of the dilution ratio in **Fig. 6**. These data have been fitted to **Eq. 2** obtaining as the only adjustable parameter the histamine concentration in wine, which is found to be 4.5±0.1 μM, a value in agreement to the average value of histamine content in white wines [26].

Wine is a matrix that presents a high number of potentially interfering species, because it is characterized by a complex chemical composition [31]. In this respect, the presence of ionic species is critical because the presence of counterions of a charged colloidal dispersion (cations in the present case) screens the charges on the particles and above the so-called *critical coagulation concentration* (*ccc*) eventually destabilizes the dispersion. According to the DLVO theory, the *ccc* value depends on the cation valency (*z*) according to [32]:

$ccc\ (M) = \frac{87.4 \cdot 10^{-40}}{z^6 H^2} = \frac{55 \cdot 10^{-3}}{z^6}$. The last equality is obtained considering the Hamaker constant of gold *H*~ 100 k_bT [33]. Accordingly, the expected *ccc* are ~ 50 mM for monovalent and 800 μM for divalent cations. Typical concentration of Ca^{2+}, Na^{+}, Mg^{2+} in white wines are below 200 mg/L while the potassium, K^{+}, can be present in higher concentrations, up to 1000 mg/L [34,35,36]. In any case a 1/10 dilution should be enough to push the cation concentrations below their *ccc* avoiding any interference in the assay.

4. Conclusions

In this study, we have exploited gold nanoparticles prepared by laser ablation and therefore free from any capping agent to demonstrate that biogenic amines (histamine in the present case) induce the nanoparticle aggregation through non-electrostatic interaction with the gold surface. The dependence of the aggregate size on the ratio amine/nanoparticle indicates that histamine acts as bidentate ligand able to crosslink two particles at time. Under suitable concentrations, the number of bound ligands and of free binding-sites is large enough to obtain the crosslinking of several nanoparticles with a concomitant change in the sample color from burgundy to blue gray. In the case of AuNP at a concentration of 1 nM, the solution turns gray for histamine concentration above few tenths of micromolar.

We have developed a robust analytical assay for BAs based on the use as response of the ratio of the absorbance values at three wavelengths: (Abs @650 nm + Abs@900 nm])/ Abs@520 nm (Aggregation Index). Quantification of the BA content is achieved by comparing the unknown responses along the dilution path with the response upon dilution of a solution of histamine of known concentration. The assay was successfully tested on a real sample of wine.

Acknowledgments

Partial financial support by the Center for Colloid and Surface Science (CSGI) is acknowledged. We also thank Prof. Alessandro De Giacomo for helpful discussions.

References

[1] M. Papageorgiou, D. Lambropoulou, C. Morrison, E. Kłodzinska, J. Namiesnik, J. Płotka-Wasylka, Literature update of analytical methods for biogenic amines determination in food and beverages, TrAC 98 (2018) 128e142. https://doi.org/10.1016/j.trac.2017.11.001
[2] F.B. Erim, Recent analytical approaches to the analysis of biogenic amines in food samples, TrAC 52 (2013) 239–247. http://dx.doi.org/10.1016/j.trac.2013.05.018
[3] M. Gagic, E. Jamroz, S. Krizkova, V. Milosavljevic, P. Kopel, V. Adam, Current Trends in Detection of Histamine in Food and Beverages, J. Agric. Food Chem. 67 (2019) 773−783. https://doi.org/10.1021/acs.jafc.8b05515
[4] C.C. Chang, C.P. Chen, T.H. Wu, C.H. Yang, C.W. Lin, C.Y. Chen, Gold Nanoparticle-Based Colorimetric Strategies for Chemical and Biological Sensing Applications, Nanomaterials, 9 (2019) 861. https://doi.org/10.3390/nano9060861.
[5] H. Aldewachi, T. Chalati, M.N. Woodroofe, N. Bricklebank, B. Sharrackc and P. Gardiner, Gold nanoparticle-based colorimetric biosensors, Nanoscale, 10 (2018) 18-33. https://doi.org/10.1039/c7nr06367a

[6] A.E. Urusov, A.V. Petrakova, P.G. Kuzmin, A.V. Zherdev, P.G. Sveshnikov, G.A. Shafeev, B.B. Dzantiev, Application of gold nanoparticles produced by laser ablation for immunochromatographic assay labeling, Anal. Biochem., 491 (2015) 65-71. https://doi.org/10.1016/j.ab.2015.08.031
[7] A. Moyano, M. Salvador, J.C. Martínez-García, V. Socoliuc, L. Vékás, D. Peddis, M.A. Alvarez, M. Fernández, M. Rivas, M.C. Blanco-López, Magnetic immunochromatographic test for Histamine detection in wine, Anal. Bioanal. Chem., 411 (2019) 6615–6624. https://doi.org/10.1007/s00216-019-02031-6
[8] C. Huang, S. Wang, W. Zhao, C. Zong, A. Liang, Q. Zhang, X. Liu, Visual and photometric determination of Histamine using unmodified gold nanoparticles, Microchim Acta 184 (2017) 2249–2254. https://doi.org/10.1007/s00604-017-2253-9
[9] K.M.A. El-Nour, E.T.A. Salam, H.M. Soliman and A.S. Orabi, Gold Nanoparticles as a Direct and Rapid Sensor for Sensitive Analytical Detection of Biogenic Amines, Nanoscale Research Letters 12 (2017) 231. https://doi.org/10.1186/s11671-017-2014-z
[10] C.F. Chow, Biogenic amines- and sulfides-responsive gold nanoparticles for real-time visual detection of raw meat, fish, crustaceans, and preserved meat, Food chemistry, 311 (2020) 125908. https://doi.org/10.1016/j.foodchem.2019.125908
[11] N. Mohseni, M. Bahram, Highly selective and sensitive determination of dopamine in biological samples via tuning the particle size of label-free gold nanoparticles, Spectrochimica Acta Part A: Molecular and Biomolecular Spectroscopy 193 (2018) 451–457. https://doi.org/10.1016/j.saa.2017.12.033
[12] N. Gao, P. Huang, F. Wu, Colorimetric detection of melamine in milk based on Triton X-100 modified gold nanoparticles and its paper-based application, Spectrochimica Acta Part A: Molecular and Biomolecular Spectroscopy 192 (2018) 174–180. https://doi.org/10.1016/j.saa.2017.11.022
[13] N. Kumar, R. Seth, H. Kumar, Colorimetric detection of melamine in milk by citrate-stabilized gold nanoparticles, Anal. Biochem., 456 (2014) 43–49. http://dx.doi.org/10.1016/j.ab.2014.04.002
[14] D. Zhang, B. Gökce, S. Barcikowski, Laser Synthesis and Processing of Colloids: Fundamentals and Applications, Chem. Rev., 117 (2017) 3990-4103. https://doi.org/10.1021/acs.chemrev.6b00468
[15] M. Dell'Aglio, R. Gaudiuso, O. De Pascale, A. De Giacomo, Mechanisms and processes of pulsed laser ablation in liquids duringnanoparticle production Applied Surface Science, 348 (2015) 4-9. http://dx.doi.org/10.1016/j.apsusc.2015.01.082
[16] A.A. Serkov, E.V. Barmina, A.V. Simakin, P.G. Kuzmin, V.V. Voronov, G.A. Shafeev, Generation of core-shell nanoparticles Al@Ti by laser ablation in liquid for hydrogen storage, Applied Surface Science, 348 (2015) 71-74. https://doi.org/10.1016/j.apsusc.2015.02.044
[17] N.A. Aksenova, M.A. Savko, O.Y. Uryupina, V.I. Roldugin, P.S. Timashev, P.G. Kuzmin, G.A. Shafeev, A.B. Soloveva, Effect of the preparation method of silver and gold nanoparticles on the photosensitizing properties of tetraphenylporphyrin–amphiphilic polymer—nanoparticle systems, Russian Journal of Physical Chemistry A, 91 (2017) 124-129. https://doi.org/10.1134/S0036024417010022
[18] X. Liu, Q. Han, Y. Zhang, X. Wang, S. Cai, C. Wang, R. Yang, Green and facile synthesis of Rh/GO nanocomposites for high catalytic performance, Applied Surface Science, Volume 471, 2019, pp. 929-934. https://doi.org/10.1016/j.apsusc.2018.12.065
[19] G. Shafeev, E. Barmina, L. Valiullin, A. Simakin, A. Ovsyankina, D. Demin, V. Kosolapov, A. Korshunov, R. Denisov, Soil fertilizer based on selenium nanoparticles, IOP Conference Series: Earth and Environmental Science, 390 (2019) (1), art. no. 012041.
[20] M. Rodio, L. Coluccino, E. Romeo, A. Genovese, A. Diaspro, G. Garau, R. Intartaglia, Facile fabrication of bioactive ultra-small protein–hydroxyapatite nanoconjugates via liquid-phase laser ablation and their enhanced osteogenic differentiation activity, J. Mater. Chem. B, 5 (2017) 279-288. https://doi.org/10.1039/c6tb02023b
[21] M. I. Zhil'nikova, E. V. Barmina, and G. A. Shafeev, Laser-Assisted Formation of Elongated Au Nanoparticles and Subsequent Dynamics of Their Morphology under Pulsed Irradiation in Water, Physics of Wave Phenomena, 2018, Vol. 26, No. 2, pp. 85-92. https://doi.org/10.3103/S1541308X18020024
[22] H. Mateos, A. Valentini, E. Robles, A. Brooker, N. Cioffi, G. Palazzo, Measurement of the zeta-potential of solid surfaces through Laser Doppler Electrophoresis of colloid tracer in a dip-cell: Survey of the effect of ionic strength, pH, tracer chemical nature and size, Colloids Surf. A, *576* (2019) 82–90. https//doi.org/10.1016/j.colsurfa.2019.05.006
[23] M. Dell'Aglio, V. Mangini, G. Valenza, O. De Pascale, A. De Stradis, G. Natile, F. Arnesano, A. De Giacomo, Applied Surface Science 374 (2016) 297–304.
[24] T. Surya, B. Sivaraman, V. Alamelu, A. Priyatharshini, U. Arisekar and S. Sundhar, Rapid Methods for Histamine Detection in Fishery Products, Int. J. Curr. Microbiol. App. Sci, 8 (2019) 2035-2046. https://doi.org/10.20546/ijcmas.2019.803.242
[25] S. Yadav, S.S. Nair, V.V.R. Sai, J. Satija, Nanomaterials based optical and electrochemical sensing of Histamine: Progress and perspectives, Food Research International 119 (2019) 99–109. https://doi.org/10.1016/j.foodres.2019.01.045

[26] F. Esposito, P. Montuori, M. Schettino, S. Velotto, T. Stasi, R. Romano and T. Cirillo, Level of Biogenic Amines in Red and WhiteWines, Dietary Exposure, and Histamine-Mediated Symptoms upon Wine Ingestion, Molecules, 24 (2019) 3629. https://doi:10.3390/molecules24193629
[27] J. Turkevich, P.C. Stevenson, J. Hillier, A study of the nucle-ation and growth processes in the synthesis of colloidal gold, Discuss Faraday Soc, 11 (1951) 55–75. doi:10.1039/df9511100055
[28] G.R. Souza, C.S. Levin, A. Hajitou, R. Pasqualini, W. Arap, J.H. Miller, In Vivo Detection of Gold-Imidazole Self-Assembly Complexes: NIR-SERS Signal Reporters, Anal. Chem. 78 (2006) 6232-6237. http://dx.doi.org/10.1021/ac060483a
[29] S.K. Ghosh, S. Nath, S. Kundu, K. Esumi, T. Pal, Solvent and Ligand Effects on the Localized Surface Plasmon Resonance (LSPR) of Gold Colloids, J. Phys. Chem. B, 108 (2004) 13963-13971. http://dx.doi.org/10.1021/jp047021q
[30] Schreiber, G.; Haran, G.; Zhou, H. X. *Chem. Rev.* **2009**, *109*, 839-860. doi: 10.1021/cr800373w
[31] M. Butnariu, A. Butu, Qualitative and quantitative chemical composition of wine, Quality Control in the Beverage Industry, In: Quality Control in the Beverage Industry, 385-41 (2019). https://doi.org/10.1016/B978-0-12-816681-9.00011
[32] R.J. Hunter, *Zeta potential in colloidal science*, Academic Press, 2013.
[33] J.N. Israelachvili, *Intermolecular and Surface Forces*, Elsevier, 2011, ISBN 9780123751829
[34] V.F. Laurie, E. Villagra, J. Tapia, J.E.S. Sarkis, M.A. Hortellani, Analysis of major metallic elements in Chilean wines by atomic absorption spectroscopy, Cienc. Inv. Agr., 37 (2010) 77-85. http://dx.doi.org/10.4067/S0718-16202010000200008
[35] M. Olalla, M.C. Gonzales, C. Cabrera, R. Gimenez, M.C. Lopez, Optimized Determination of Calcium in Grape Juice, Wines, and Other Alcoholic Beverages by Atomic Absorption Spectrometry, J. AOAC Int., 85 (2002) 960-966.
[36] A. Cabello-Pasini, V. Macias-Carranza, A. Siqueiros-Valencia, M.A. Huerta-Diaz, Concentrations of Calcium, Magnesium, Potassium, and Sodium in Wines from Mexico, Am. J. Enol. Vitic. 64 (2013) 280-284.